Synthesis of PEDOT Nano-objects Using Poly(vinyl alcohol)-Based Reactive Stabilizers in Aqueous Dispersion

Muhammad Mumtaz,[†,‡] **Emmanuel Ibarboure,**[†,‡]
Christine Labrugère,[§] **Eric Clouet,**[*,†,‡] **and**
Henri Cramail[*,†,‡]

*Laboratoire de Chimie des Polymères Organiques, CNRS,
16 avenue Pey Berland, Pessac Cedex F33607, France;
Laboratoire de Chimie des Polymères Organiques,
Université de Bordeaux, ENSCPB, Pessac Cedex F33607,
France; and Institut de Chimie de la Matière Condensée de
Bordeaux, CNRS, 87 avenue du Docteur Schweitzer,
Pessac Cedex F33608, France*

Conducting polymers are an attractive class of materials that combine the general properties of traditional organic polymers with the electrical conductivity of metals or semiconductors. They have potential applications in electrochromics,[1] supercapacitors,[2] antistatic and electrostatic coatings,[3] light-emitting devices,[4,5] photovoltaics,[6] sensors,[7] etc. However, their insolubility in some solvents limits their wider use. One method to improve the processability of these polymeric materials is by preparing them in water-borne or organic dispersions. This process may have considerable environmental and economic advantages for large scale concerns. Aqueous dispersions of polypyrrole and polyaniline have been already prepared by chemical oxidative polymerization of the corresponding monomers in the presence of suitable water-soluble steric stabilizers.[8–16] Among conducting polymers, poly(3,4-ethylenedioxythiophene) (PEDOT) has been well investigated due to its good environmental stability, low band gap, low redox potential, and high optical transparency in its electrically conductive state, all properties that make it an excellent candidate for use in optoelectronics.[17–19] Despite the fact that the PEDOT–poly-(styrenesulfonate) (PEDOT–PSS) mixture is largely used for photovoltaics, there is still a need to optimize the synthesis and the morphology of PEDOT in order to tune the optoelectronic properties.

Many groups have reported different techniques to synthesize PEDOT nano-objects with the aim of improving its processability.[20–26] Recently, Sun et al. reported the synthesis of PEDOT nanowires in the presence of poly(acrylic acid).[27] We also described the synthesis of PEDOT nanoparticles and vesicles by dispersion polymerization of EDOT in alcoholic media in the presence of reactive poly(ethylene oxide) end-capped with EDOT, fluorene, pyrrole (Py), and thiophene functions.[28,29]

In this Communication, we discuss the synthesis in aqueous dispersion of well-defined PEDOT nano-objects with various morphologies, including particles and donuts, in the presence of Py-grafted poly(vinyl alcohol) (PVA-*g*-Py) used as a reactive stabilizer. Ammonium persulfate and iron(III) *p*-toluenesulfonate hexahydrate [Fe(III)(OTs)$_3$·6(H$_2$O)] were tested as oxidants.

The nano-objects formed show electrical conductivity up to 1.6×10^{-2} S cm^{-1}. The size of these nano-objects ranges from 30 to 200 nm (excepting in the case of doughnuts) depending upon the experimental conditions.

3,4-Ethylenedioxythiophene (EDOT), *N*-methyl-2-pyrrole-carboxylic acid, and poly(vinyl alcohol) (PVA) were purchased from Aldrich and used without further purification. Dimethyl sulfoxide (DMSO) was distilled over CaH$_2$. Ammonium persulfate, iron(III) *p*-toluenesulfonate hexahydrate [Fe(III)(OTs)$_3$·6(H$_2$O)] of technical grade, and *p*-toluenesulfonic acid (98.5%) were purchased from Aldrich and used as received. 4-(Dimethylamino)pyridinium 4-toluenosulfonate (DPTS) was prepared as described in the literature.[30]

In a typical procedure, PEDOT particles of 180–200 nm diameter were prepared by dispersion polymerization as following: (PVA-*g*-Py) (270 mg, $\bar{M}_w = 18\,000$ g mol^{-1}) (see its synthesis in Supporting Information (SI)) was introduced in a 250 mL flask equipped with a mechanical stirrer. A mixture (1:4, v/v) of methanol and water (40 mL) was then added, and the temperature of the system was raised up to 60 °C in order to dissolve the stabilizer. The temperature was then lowered to 40 °C, and EDOT (0.5 g, 3.5 mmol) was charged in the flask in one shot. A solution of ammonium persulfate (1.30 g dissolved in 10 mL of 1:4 methanol–water mixture) was then introduced in a single dose. The reaction mixture was stirred for 72 h at room temperature. The resulting blue dispersion was centrifuged at 10 000 rpm at 5 °C for 30 min. The supernatant was carefully decanted and the dark blue sediment was redispersed in methanol/water mixture. This redispersion–centrifugation cycle was repeated three times in order to ensure the complete removal of inorganic material such as ammonium sulfate and eventual unattached reactive stabilizer.

^{1}H NMR spectra were recorded using a Bruker AC-400 NMR spectrometer. Conductivity measurements of the PEDOT samples (pressed pellets) were performed using a Keithley 2400 Source Meter four-probe instrument. SEM images of the PEDOT samples were taken using a JEOL JSM-5200 scanning microscope. Atomic force microscopy (AFM) images were recorded in air with a Nanoscope IIIa microscope operating in tapping mode (TM). The probes were commercially available as silicon tips with a spring constant of 42 N m^{-1}, resonance frequency of 285 kHz, and a typical radius of curvature in the 10–12 nm range. Both the topography and the phase signal images were recorded with a resolution of 512×512 data points. Samples for AFM were prepared by solvent casting at room temperature from water/methanol solutions. Typically, 100 μL of a dilute solution (0.1 wt %) was cast on a 1×1 cm^2 freshly cleaved mica. Dynamic light scattering (DLS) measurements were performed at 25 °C using an ALV laser goniometer. TGA measurements were taken using Perkin-Elmer thermogravimetric analyzer (TGA 7). XPS measurements were made using an ESCALAB 220-iXL spectrometer (Thermo-Electron, VG Co.). Photoemission was stimulated by a monochromatized Al Kα radiation (1486.6 eV). An area of about 250 μm diameter was analyzed for each sample. Surveys and high-resolution spectra were recorded and then fitted with an Avantage processing program provided by ThermoFisher Scientific. UV–vis spectra were recorded with a Spectramax-M2 spectrometer. Infrared measurements (FTIR) spectra were performed on a Bruker Tensor 27 spectrometer.

In order to prepare PEDOT core–shell particles, we derivatized a series of PVA-*g*-Py (that are used as steric reactive
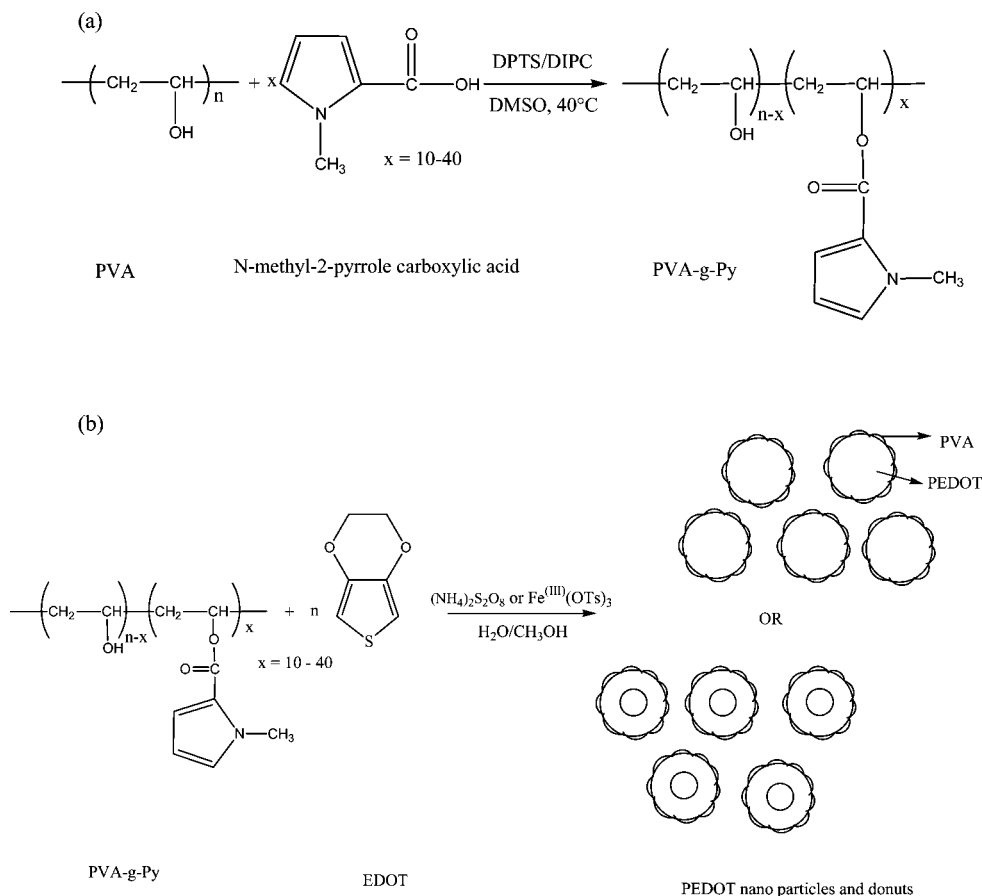
* Corresponding authors. E-mail: cloutet@enscpb.fr (E.C.); cramail@enscpb.fr (H.C.).
† Laboratoire de Chimie des Polymères Organiques, CNRS.
‡ Université de Bordeaux.
§ Institut de Chimie de la Matière Condensée de Bordeaux, CNRS.

Scheme 1. (a) Synthesis of PVA-*g*-Py and (b) Synthesis of PEDOT Particles and Donuts

stabilizers) with different degrees of substitution and molar mass by partial esterification of PVA with *N*-methyl-2-pyrrolecarboxylic acid in the presence of 4-(dimethylamino)pyridinium 4-toluenesulfonate (DPTS).[30] The general synthetic procedure is shown in Scheme 1.

^{1}H NMR of the PVA-*g*-Py in DMSO is shown in Figure 1. The appearance of the signals at 7.05 (h), 6.80 (f), and 6.07 ppm (g) due to pyrrole ring resonance confirmed the grafting of pyrrole units along the PVA backbone. ^{1}H NMR analysis was used to evaluate the density of grafting of pyrrole units per PVA chain in particular for degree of substitution higher than 5%.

In order to improve the solubility of EDOT in water, the dispersion polymerization was performed in a mixture of methanol:water (1:4). Two types of oxidants, i.e., ammonium persulfate and Fe[(III)](OTs)$_3$·6(H$_2$O), were used for the oxidative polymerization of EDOT. The effect of the concentration, degree of substitution, and the molar mass of the PVA-*g*-Py stabilizers on the morphology and size of the nano-objects was investigated and analyzed by dynamic light scattering (DLS). The data of EDOT dispersion polymerization in the presence of PVA-*g*-Py are summarized in Table 1.

Unlike polymerizations of EDOT performed in the presence of nonmodified PVA (run 1), the grafting of PVA hydroxyl moieties with pyrrole was shown to be essential in order to prepare PEDOT nano-objects having various morphologies (runs 2–15) (see Figure SI1).

Above 5 mol %, the degree of PVA substitution ([Py]) has a little effect on the average PEDOT particle size which remains in the range 100–200 nm (runs 5–15). However, at a very low degree of substitution (runs 3 and 4), there is an amazing formation of rings, or so-called "donuts" (for more images see

Figure SI7). Although we do not have a full explanation on the formation of donuts, there is an evident relationship between the density of pyrrole grafting onto the PVA reactive stabilizers and the morphology of PEDOT objects. A lack of thermody-
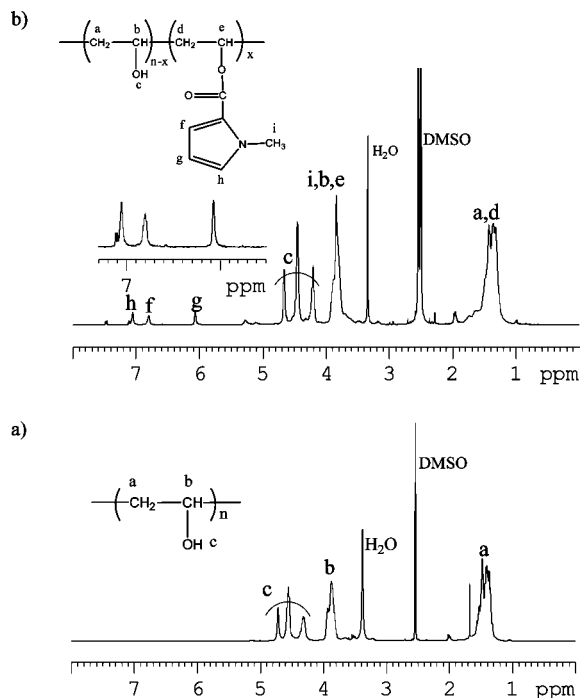

Figure 1. ^{1}H NMR spectra of (a) PVA and (b) PVA-*g*-Py in DMSO at room temperature.

Table 1. Synthesis of PEDOT Particles Using PVA-*g*-Py as a Reactive Stabilizer in Water/Methanol (1:4) at 40 °C

run no.	oxidant type	PVA-*g*-Py M_w (g mol^{-1})	mol % of Py per chain	PVA-*g*-Py introduced (wt %)	yield (%)	conductivity[a] (S cm^{-1})	particle size[b] (nm)	remarks
1	$(NH_4)_2S_2O_8$	18 000	0	20	50	nd	−	aggregates
2	$(NH_4)_2S_2O_8$	18 000	2.5	20	55	nd	−	aggregates
3	$(NH_4)_2S_2O_8$	18 000	2.5	35	60	3.5×10^{-6}	300−400	donuts
4	$(NH_4)_2S_2O_8$	18 000	5.0	20	70	3.2×10^{-6}	400−800	donuts
5	$(NH_4)_2S_2O_8$	18 000	5.0	35	60	7.5×10^{-5}	180−200	particles
6	$(NH_4)_2S_2O_8$	18 000	7.5	10	55	9.0×10^{-6}	150−180	particles
7	$(NH_4)_2S_2O_8$	18 000	7.5	20	60	3.6×10^{-6}	100−140	particles
8	$(NH_4)_2S_2O_8$	18 000	7.5	35	50	1.6×10^{-6}	80−120	particles
9	$(NH_4)_2S_2O_8$	18 000	10.0	20	60	7.2×10^{-6}	150−200	particles
10	$(NH_4)_2S_2O_8$	88 000	1.0	10	60	4.4×10^{-6}	150−190	particles
11	$(NH_4)_2S_2O_8$	88 000	1.0	20	50	4.0×10^{-6}	100−170	particles
12	$(NH_4)_2S_2O_8$	88 000	5.0	10	60	nd	80−100	particles
13	$(NH_4)_2S_2O_8$	88 000	5.0	20	60	nd	50−100	particles
14[c]	Fe(OTs)$_3$	88 000	5.0	35	80	1.6×10^{-2}	100−140	particles
15[c]	Fe(OTs)$_3$	18 000	7.5	50	80	1.8×10^{-3}	50−60	particles

[a] Measured by the four probe method. [b] Measured from SEM images. In all cases averages on 100 objects were made. [c] Reaction mixture kept at 85 °C for 48 h.
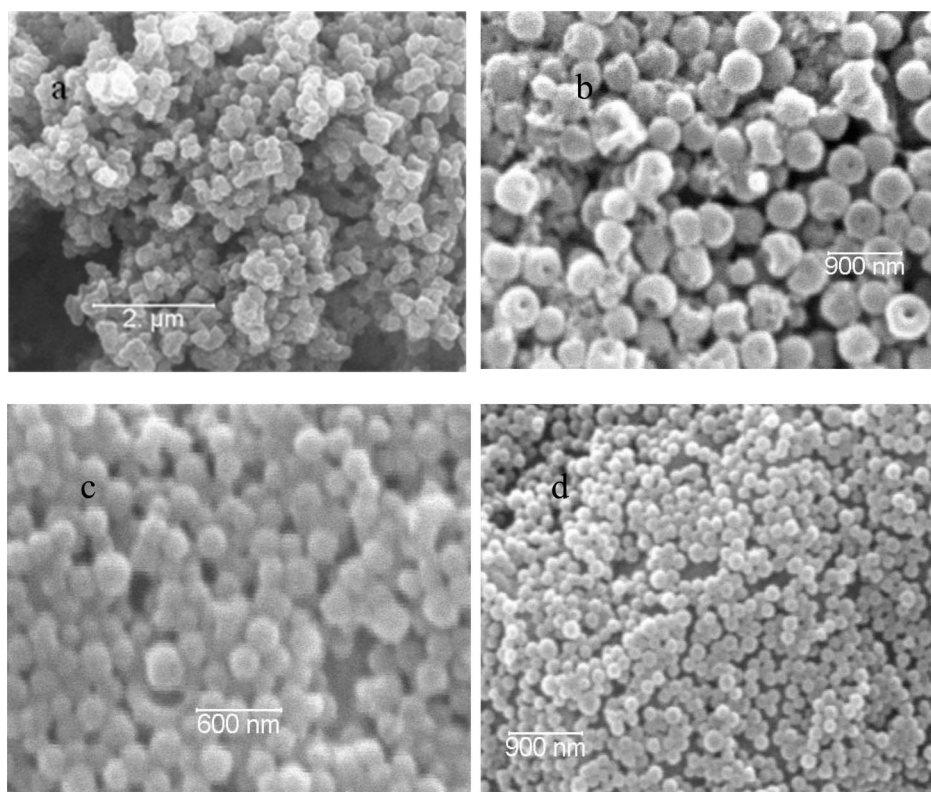

Figure 2. SEM images of PEDOT particles and donuts prepared using different PVA-*g*-Py stabilizers with various degrees of pyrrole grafting and concentrations: (a) 2.5% of Py grafting, 20 wt % (run 2); (b) 5% of Py grafting, 20 wt % (run 4); (c) 10% of Py grafting, 20 wt % (run 9); (d) 5% of Py grafting, 35 wt % (run 5).

namic stability is probably the cause of the formation of hollow spheres. It is noteworthy that ring structure have been already reported by Dìez et al. in the case of synthesis of polypyrrole in aqueous media.[31] However, in this specific work the authors use templates (β-naphthalene and fluorosurfactants) for pyrrole polymerization. In our case, we have checked by DLS measurements that no particular self-organization of the PVA-*g*-Py reactive stabilizer was formed prior polymerization. The change in PEDOT morphologies from donuts to dense particles was noticed while increasing the concentration of pyrrole units onto PVA backbone (see runs 3 and 5). Spherical particles were only obtained above a critical value of pyrrole units as it is illustrated in Figures 2 and 3.

In accordance with literature data,[9,32] the average size of the PEDOT particles decreases from 170 to 100 nm as the concentration in stabilizer increases from 10 to 35 wt % (see

runs 6−8 and 10, 11). This is logically explained by a higher surface coverage in the presence of a higher amount of steric reactive stabilizer (see Figure SI3c,d).

As expected, the molar mass of the stabilizer also affects the size of the PEDOT particles. The latter decreases as the molar mass of the PVA-*g*-Py increases from 18 000 to 88 000 g mol^{-1}, even at low stabilizer concentrations (see runs 4, 5, 12, and 13). This is again explained by the higher surface coverage afforded by the high molar mass stabilizer molecules, which leads to the formation of a larger number of stable primary particles. Similar results were obtained and reported by Mandal and colleagues for the dispersion polymerization of pyrrole.[11]

AFM images (Figure 3) (for more images see Figure SI2) clearly show that each PEDOT nano-object is formed by the aggregation of the very small nanoparticles having a size
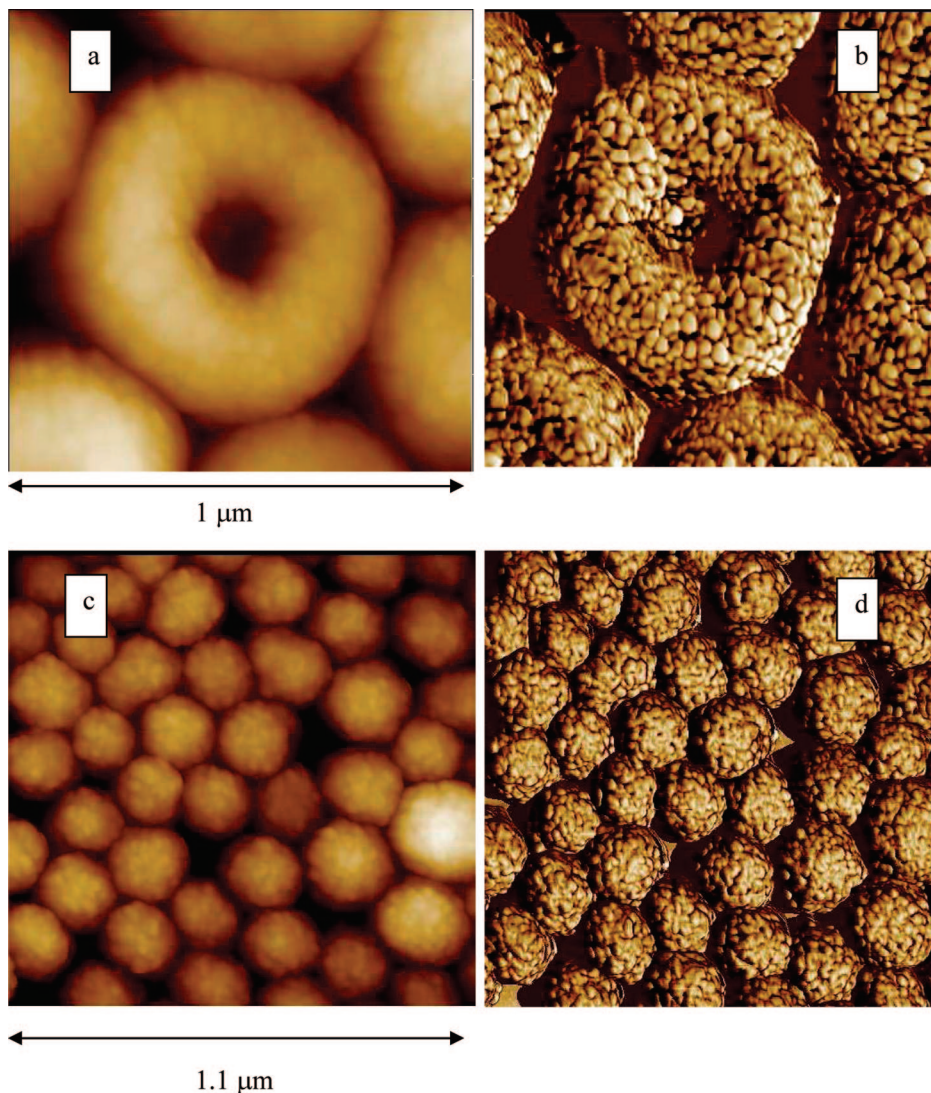
Figure 3. AFM images of PEDOT particles and donuts prepared using PVA-*g*-Py stabilizer having 5 mol % of pyrrole grafting, at different concentrations: (a, b) 20 wt % (rn 4); (c, d) 35 wt % (run 5).

between 20 and 30 nm which were also called particulates or metastable particles by Mandal and colleagues.[33] These results thus further strengthen the mechanism of the particle formation given by Paine that each large stable particle is formed by the combination of small metastable elementary particles.[34−36] Similar results were observed and reported later by Armes et al. with the help of scanning tunneling microscopy.[32]

As already noted,[28,29] PEDOT particles were obtained in high yield when using $Fe^{(III)}(OTs)_3 \cdot 6(H_2O)$ as an oxidant at 85 °C (see runs 14 and 15). This is explained by a higher efficiency of $Fe^{(III)}(OTs)_3.6(H_2O)$ in the given experimental conditions as compared to ammonium persulfate. In addition, the PEDOT particles formed in these conditions are smaller in size as compared to the ones obtained using ammonium persulfate as an oxidant for a same degree of substitution and concentration of stabilizer (see runs 5 and 14). The PEDOT samples synthesized in the presence of $Fe^{(III)}(OTs)_3 \cdot 6(H_2O)$ are insoluble in any common organic solvent, preventing their characterization by NMR and SEC.

The conductivity of the PEDOT particles was measured using the conventional four-probe technique on dried and compressed PEDOT powders under the form of disk pellets. PEDOT samples prepared using ammonium persulfate as an oxidant show low conductivities (up to 9.0×10^{-6} S cm^{-1}) while those

prepared using $Fe^{(III)}(OTs)_3 \cdot 6(H_2O)$ exhibit higher conductivities (up to 1.6×10^{-2} S cm^{-1}). This is explained by the higher content and molar mass of PEDOT within the latter samples and also because in case of ammonium persulfate PEDOT samples are overoxidized.

In order to further analyze the size, size distribution, and morphology of PEDOT nano-objects, dynamic light scattering (DLS) experiments of PEDOT samples were performed in methanol/water (1:4) mixture. DLS results for a PEDOT sample (run 5) are shown in Figure SI4.

The autocorrelation functions $C(q,t)$ (Figure SI4a) and the corresponding relaxation time distributions $G(t)$ (Figure SI4b) of a PEDOT sample measured at different angles show a single population with very narrow relaxation time distributions in each case. This confirms that PEDOT nano-objects have very narrow size distribution which was already illustrated by AFM images. The evolution of the relaxation frequency as a function of the square of the wave vector permits us to calculate the apparent diffusion coefficient of PEDOT particles. The linear relation between relaxation frequency and square of the wave vector (Figure SI4c) confirms the homogeneous size and spherical nature of these PEDOT nano-objects. The size of these latter particles was found to be 200 nm, which is in agreement with the results obtained by AFM and SEM. These DLS results
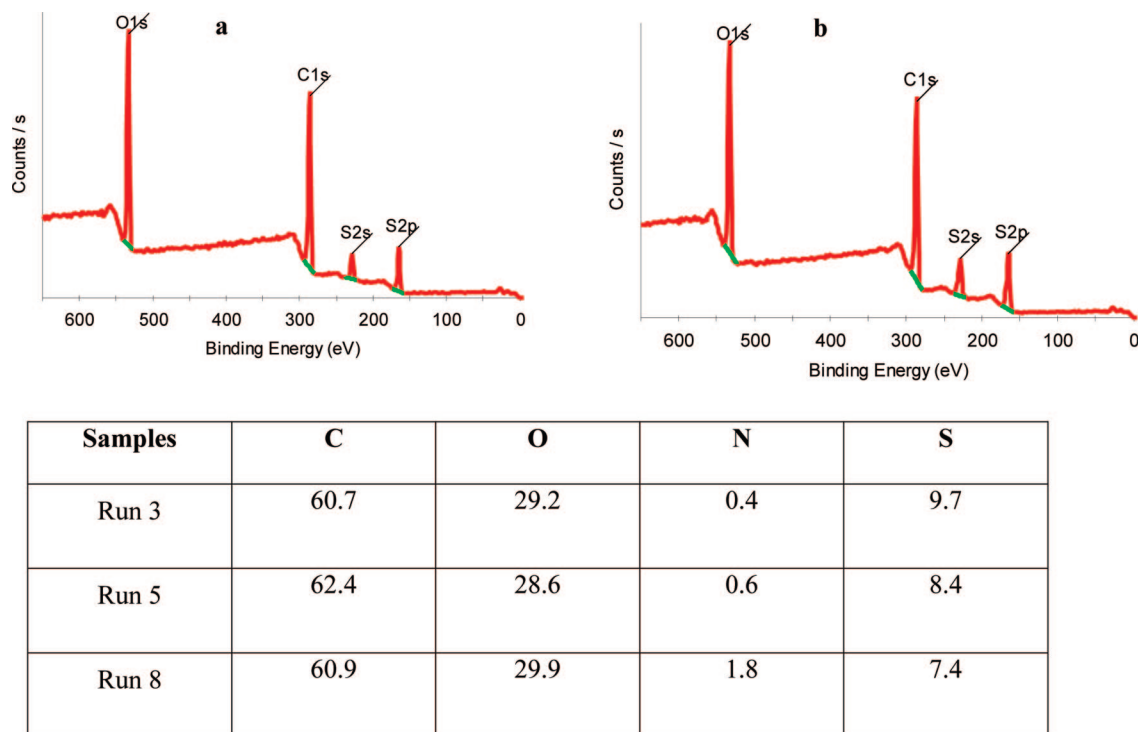
Samples	C	O	N	S
Run 3	60.7	29.2	0.4	9.7
Run 5	62.4	28.6	0.6	8.4
Run 8	60.9	29.9	1.8	7.4

Figure 4. XPS survey spectra of (a) PEDOT core−shell particles and (b) PEDOT bulk powder. (c) Table for the estimation of chemical composition on surface of PEDOT−PVA samples.

further prove that these particles are monodispersed and are well separated from each other; i.e., no aggregation occurs among final PEDOT particles.

The core−shell nature of the formed particles, i.e. shell of PVA onto PEDOT core, was proved by X-ray photoelectron microscopy (XPS) analyses. XPS survey spectra of PEDOT core−shell particles and PEDOT bulk powder are presented in Figure 4. Both samples show four peak signals originating from C 1s, O 1s, S 2s, and S 2p. The relative intensity of the signals due to S 2s and S 2p in PEDOT core−shell particles is lower than PEDOT bulk powder. In addition, XPS analyses allowed us to estimate the surface coverage of the PEDOT particles by the PVA stabilizer as revealed for instance by the presence of the N 1s signal. As anticipated, data gathered in Figure 4c reveal an increase of the N% together with the expected mol % of pyrrole groups per chain. For runs 3 and 5, the binding energy of the maximum at 399.9 eV is consistent with the *N*-methylpyrrole groups on the PVA stabilizer chains (see also Figure SI5a,b). For run 8, the N 1s maximum is located at 401.4 eV, suggesting some remaining ammonium ions from $(NH_4)_2S_2O_8$ onto the particles (Figure SI5c).

In addition, Figure 5a,b shows the C 1s core-line spectra of PEDOT core−shell particles and PEDOT bulk powder. The peak at 286.4 eV position in C 1s core-line spectra of PEDOT core−shell particles corresponds to C−O−H moieties in PVA.[37−39] In addition, the presence of peak at 532.6 eV (Figure 5c) originating from O 1s is due to C−O−H and is in agreement with the data already available in the literature.[37] Such a peak was not observed in O 1s core-line spectrum of PEDOT bulk powder (Figure 5d), which confirms the presence of PVA on the PEDOT surface of PEDOT core−shell particles. The S 2p core-line spectra of the samples are shown in Figure 5e,f. The peaks at 164−165.2 eV correspond to neutral S of PEDOT backbone while the peaks at 167.6−168.9 eV are due to sulfate anions.[40] The signals at 165.8−167.2 eV due to S+ of PEDOT were difficult to observe in PEDOT core−shell particles

probably due to the presence of the PVA shell. Finally, the amount of sulfur in the PEDOT−PVA sample was 8.5% against 12% in PEDOT bulk powder, which is again in accord with the presence of PVA on the PEDOT surface.

The formation of PEDOT latexes was also confirmed by FTIR analyses (see in Figure 6 FTIR spectra of the PEDOT bulk powder and PVA stabilized PEDOT particles using different oxidants).[41,42] The occurrence of peaks at 3424 cm^{-1} (O−H stretching vibration) and 2950 cm^{-1} (C−H stretching vibration of CH_2 group of PVA) in PEDOT particles (Figure 6b,c) confirms the presence of PVA since such peaks are not seen in PEDOT bulk powder (Figure 6a).

The composition of the PEDOT core−shell particles was also determined by thermogravimetric analysis (TGA). The TGA curves for PEDOT bulk powder, PVA, and PEDOT core−shell particles are shown in Figure SI6. The TGA curves for PEDOT−PVA core−shell particles fall in between the ones of PEDOT bulk powder and PVA, which corroborates the presence of PEDOT and PVA in the PEDOT core−shell particles samples. As expected, the TGA curve for PEDOT run 12 is more close to PEDOT bulk powder as compared to PEDOT run 13 due to greater amount of PEDOT in the former.

In conclusion, we have shown that narrow distributed PEDOT nano-objects can be easily prepared in the presence of PVA-based reactive stabilizer. No stable PEDOT dispersions were formed using unmodified PVA while stable dispersions are formed using pyrrole-modified PVA, proving the key role played by the reactive stabilizer toward the formation of stable PEDOT dispersions. The morphology of these nano-objects can be tuned by changing the concentration and degree of pyrrole function of the PVA stabilizer. These results are also a clear proof of the Paine's theory for the mechanism of particles' formation in dispersion polymerization. Because of PVA nature, latexes are very stable with respect to time and exhibit interesting film-forming property that is currently under investigation. Such
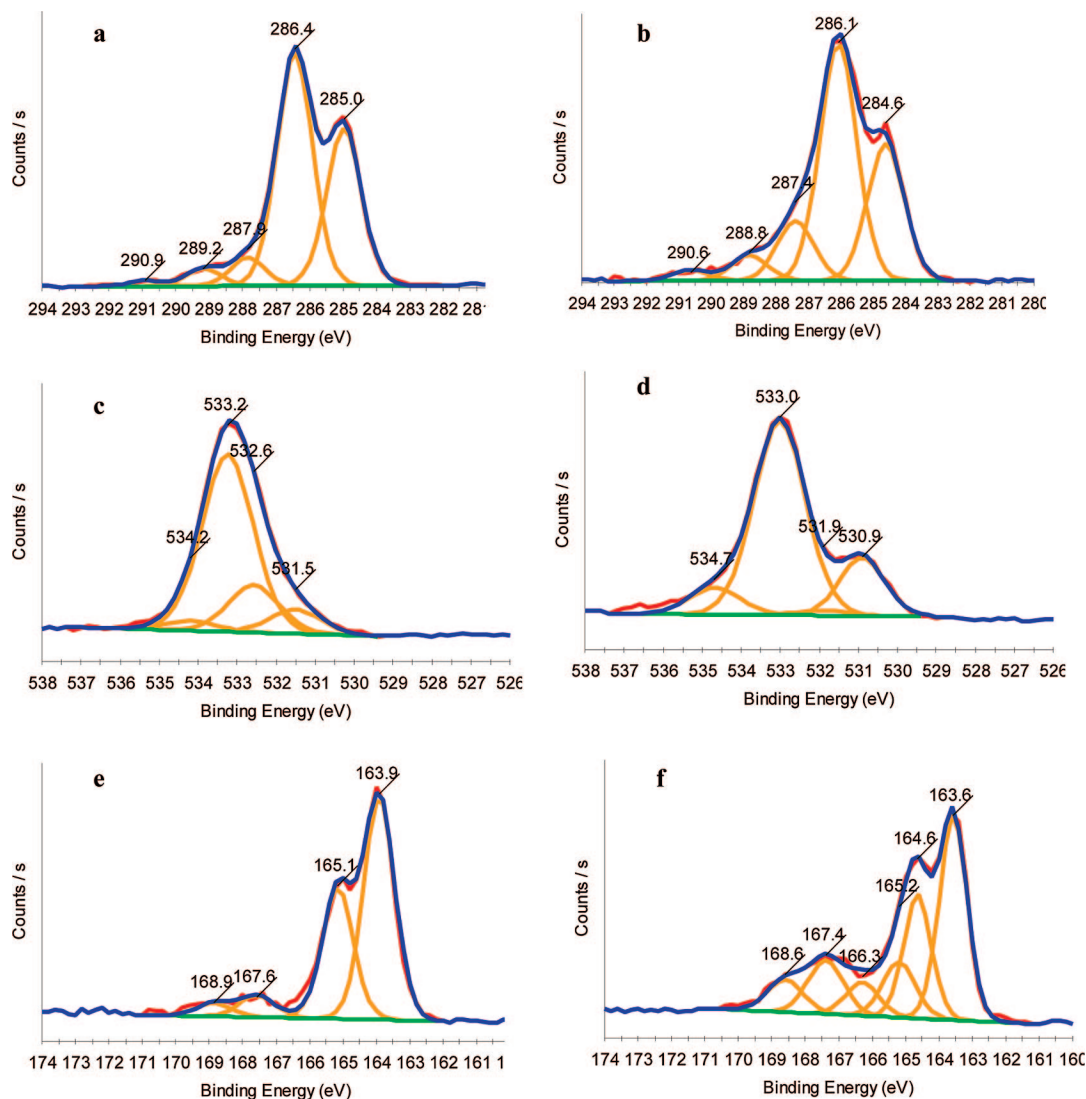
Figure 5. XPS analyses: (a, b) C 1s core-line spectra; (c, d) O 1s core-line spectra; (e, f) S 2p core-line spectra of PEDOT core−shell particles and PEDOT bulk powder, respectively.
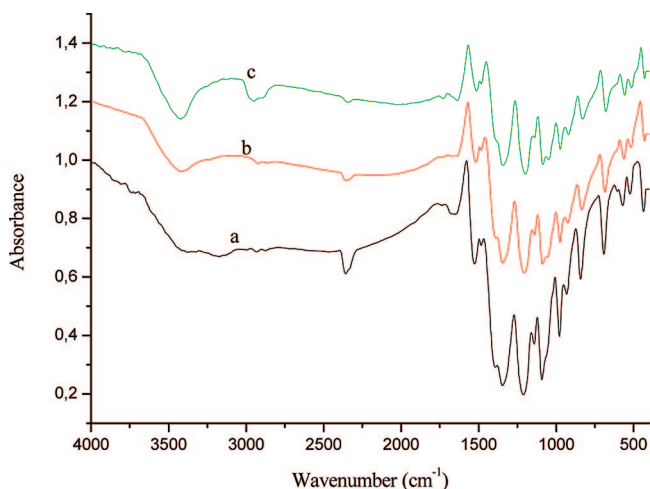
Supporting Information Available: Synthesis of poly(vinyl alcohol)-based reactive stabilizers; PEDOT latexes as obtained using (A) unmodified PVA and (B) modified PVA (PVA-*g*-Py) (Figure SI1); AFM images of PEDOT particles, donuts prepared using PVA-*g*-Py stabilizer with 5 mol % of pyrrole grafting, at different concentrations, (a) 20 wt % (run 4) and (b) 35 wt % (run 5) (Figure SI2); SEM images of PEDOT samples prepared using PVA-based stabilizers with various degrees of pyrrole substitution, concentrations, and molar mass, (a) 0% of Py grafting, 20 wt %, $\bar{M}_w = 18\ 000$ g mol^{-1} (run 1), (b) 2.5% of Py grafting, 35 wt %, $\bar{M}_w = 18\ 000$ g mol^{-1} (run 3), (c) 1% of Py grafting, 20 wt %, $\bar{M}_w = 88\ 000$ mol^{-1} (run 10), and (d) 1% of Py grafting, 35 wt %, $\bar{M}_w = 88\ 000$ g mol^{-1} (run 11) (Figure SI3); (a) autocorrelation function $C(q,t)$, (b) relaxation time distribution $G(t)$ at different angles, and (c) relaxation frequency in the function of q^2, of PEDOT sample (run 5) prepared using PVA-*g*-Py ($\bar{M}_w = 18\ 000$ g mol^{-1}, 5% pyrrole grafting) as a reactive stabilizer in water/methanol mixture (1:4) at 25 °C (Figure SI4); XPS N 1s core-line spectra for the PEDOT particles prepared using PVA-*g*-Py stabilizers having different degree of pyrrole grafting (a) 2.5 mol %, (b) 5.0 mol %, and (c) 7.5 mol % (run 3, 5, and 8, respectively) at high resolution (Ep =

Figure 6. FTIR spectra of (a) PEDOT bulk powder and (b, c) PEDOT particles prepared using Fe$^{(III)}$(OTs)$_3$·6(H$_2$O) (run 15, Table 1) and (NH$_4$)$_2$S$_2$O$_8$ (run 5, Table 1) as oxidants, respectively.

a methodology is currently investigated to prepare polyaniline and polypyrrole latexes with original morphologies. Results will be published in a forthcoming paper.

40 eV) (Figure SI5); TGA traces of PEDOT bulk powder, PVA, PEDOT run 13, and PEDOT run 12 (Figure SI6); (A) AFM and (B) TEM images of the PEDOT donuts prepared using 20 wt % of PVA-*g*-Py stabilizer having 5 mol % of pyrrole grafting (Figure SI7); details for DLS setup. This material is available free of charge via the Internet at http://pubs.acs.org.

References and Notes

(1) Welsh, D. M.; Kumar, A.; Meijer, E. W.; Reynolds, J. R. *Adv. Mater.* **1999**, *11*, 1379.

(2) Laforgue, A.; Simon, P.; Fauvarque, J. F.; Mastragostino, M.; Soavi, F.; Sarrau, J. F.; Conte, M.; Rossi, E.; Saguatti, S. *J. Electrochem. Soc.* **2003**, *150*, A645.

(3) Leeuw, D. M.; Kraakman, P. A.; Bongaerts, P. E. G.; Mutsaers, C. M. J.; Klaassen, D. B. M. *Synth. Met.* **1994**, *66*, 263.

(4) Gong, X.; Moses, D.; Heeger, A. J.; Liu, S.; Jen, A. K. Y. *Appl. Phys. Lett.* **2003**, *83*, 183.

(5) McGehee, M. D.; Heeger, A. J. *Adv. Mater.* **2000**, *12*, 1655.

(6) Gao, J.; Yu, G.; Heeger, A. J. *Adv. Mater.* **1998**, *10*, 692.

(7) Yoon, H.; Chang, M.; Jang, J. *Adv. Funct. Mater.* **2007**, *17*, 431.

(8) Armes, S. P.; Vincent, B. *J. Chem. Soc., Chem. Commun.* **1987**, 288.

(9) Armes, S. P.; Aldissi, M.; Agnew, S. F. *Synth. Met.* **1989**, *28*, 837.

(10) Simmons, M. R.; Chaloner, P. A.; Armes, S. P. *Langmuir* **1998**, *14*, 611.

(11) Mandal, T. K.; Mandal, B. M. *J. Polym. Chem., Part A: Polym. Chem.* **1999**, *37*, 3723.

(12) Pich, A.; Lu, Y.; Adler, H.-J. P.; Schmidt, T.; Arndt, K.-F. *Polymer* **2002**, *43*, 5723.

(13) Chattopadhyay, S.; Banerjee, S.; Chakravorty, D.; Mandal, B. M. *Langmuir* **1998**, *14*, 1544.

(14) Armes, S. P.; Aldissi, M.; Agnew, S.; Gottesfeld, S. *Langmuir* **1990**, *6*, 1745.

(15) Li, X.-G.; Lü, Q. F. *Chem.—Eur. J.* **2006**, *12*, 1349.

(16) Armes, S. P.; Aldissi, M.; Agnew, S.; Gottesfeld, S. *Mol. Cryst. Liq. Cryst.* **1990**, *90*, 63.

(17) Heywang, G.; Jonas, F. *Adv. Mater.* **1992**, *4*, 116.

(18) Groenendal, L.; Zotti, G.; Aubert, P.-H.; Waybright, S. M.; Reynolds, J. R. *Adv. Mater.* **2003**, *15*, 855.

(19) Imae, T.; Li, C. *Macromolecules* **2004**, *37*, 2411.

(20) Oh, S.-G.; Im, S.-S. *Curr. Appl. Phys.* **2002**, *2*, 273.

(21) Khan, M. A.; Armes, S. P. *Langmuir* **1999**, *15*, 3469.

(22) Han, M. G.; Foulger, S. H. *J. Chem. Soc., Chem. Commun.* **2004**, *19*, 2154.

(23) Müller, K.; Klapper, M.; Müllen, K. *Macromol. Rapid Commun.* **2006**, *27*, 586.

(24) Zhang, X.; Lee, J.-S.; Lee, G. S.; Cha, D.-K.; Kim, M. J.; Yang, D. J.; Manohar, S. K. *Macromolecules* **2006**, *39*, 470.

(25) Henderson, A. M. J.; Saunders, J. M.; Mrkic, J.; Kent, P.; Gore, J.; Saunders, B. R. *J. Mater. Chem.* **2001**, *11*, 3037.

(26) Han, M. G.; Armes, S. P. *Langmuir* **2003**, *19*, 4523.

(27) Sun, X.; Hanger, M. *Macromolecules* **2007**, *40*, 8537.

(28) Mumtaz, M.; de Cuendias, A.; Putaux, J.-L.; Cloutet, E.; Cramail, H. *Macromol. Rapid Commun.* **2006**, *27*, 1446.

(29) Mumtaz, M.; Lecommandoux, S.; Cloutet, E.; Cramail, H. *Langmuir* **2008**, *24*, 11911.

(30) Moore, J. S.; Stupp, S. I. *Macromolecules* **1990**, *23*, 65.

(31) Díez, I.; Tauer, K.; Schulz, B. *Colloid Polym. Sci.* **2006**, *284*, 1431.

(32) Armes, S. P.; Aldissi, M.; Hawley, M.; Beery, J. G.; Gottesfeld, S. *Langmuir* **1991**, *7*, 1447.

(33) Mandal, T. K.; Mandal, B. M. *Langmuir* **1997**, *13*, 2421.

(34) Paine, A. J. *J. Colloid Interface Sci.* **1990**, *138*, 157.

(35) Paine, A. J.; Luymes, W.; McNulty, J. *Macromolecules* **1990**, *23*, 3104.

(36) Paine, A. J. *Macromolecules* **1990**, *23*, 3109.

(37) Benseddik, E.; Makhlouki, M.; Bernede, J. C.; Lerfrant, S.; Proń, A. *Synth. Met.* **1995**, *72*, 237.

(38) Beamon, G.; Briggs, D. *High Resolution XPS of Organic Polymers*; Wiley: New York, 1992.

(39) Shakesheff, K. M.; Evora, C.; Soriano, I.; Langer, R. *J. Colloid Interface Sci.* **1997**, *185*, 538.

(40) Khan, M. A.; Armes, S. P. *Langmuir* **2000**, *16*, 4171.

(41) Yang, Y.; Jiang, Y.; Xu, J.; Yu, J. *Polymer* **2007**, *48*, 4459.

(42) Kumar, S. S.; Kumar, C. S.; Mathiyarasu, J.; Phani, K. L. *Langmuir* **2007**, *23*, 3401.

MA801856H